A Regularized Inverse Framework for Stress and Strain Analysis of Viscoelastic Bodies via DIC–FEA Integration

Yurie Rai, Keisuke Iizuka and Satoru Yoneyama

Aoyama Gakuin University, 5-10-1 Fuchinobe, Sagamihara, Japan

ABSTRACT

A method for obtaining the strain and stress distributions in a viscoelastic body is proposed by combining digital image correlation with finite element analysis based on the principle of superposition. In this method, the boundary conditions within the measurement region are determined via inverse analysis so that the computed displacement fields match those obtained experimentally. A regularization scheme is introduced to mitigate the influence of measurement errors near the boundaries. The strain distributions are obtained simultaneously with the displacement fields. Meanwhile, the streSatoruss distributions are evaluated from the temporal evolution of the strain components, taking into account the time-dependent mechanical properties of the viscoelastic material. The effectiveness of the proposed method is demonstrated through a numerical simulation. Furthermore, as an application example, stress analyses around contact interfaces are presented. The proposed method alleviates difficulties in data processing during measurement and provides an effective approach for stress and strain analysis of viscoelastic bodies.

INTRODUCTION

In recent years, the demand for lightweight and high-strength materials has led to the expansion of polymer materials into a wide range of applications. Typical examples include automobiles and aircraft, where the use of carbon fiber reinforced plastics is increasing. Polymer materials are known to exhibit viscoelastic behavior, and their mechanical properties and responses differ significantly from those of elastic materials in that they show pronounced time and temperature dependence. Therefore, applying the same treatment as for elastic materials to stress–strain analysis of viscoelastic materials often results in outcomes that are far from reality and physically meaningless. Clarifying complex phenomena such as impact, contact, and fracture in viscoelastic bodies is an important issue in both engineering and industrial contexts, and many studies have been conducted, as in the case of elastic and elastoplastic materials.[1-3]

To experimentally evaluate the mechanical behavior of solid materials, surface strain measurement is often performed. Full-field measurement methods such as moiré and digital image correlation are widely used.[4,5] These methods provide two-dimensional displacement distributions, and strain values can be obtained by differentiating the displacement distributions along the surface of the object. However, since differentiation of measured data amplifies measurement errors, it is known that special techniques are required to obtain appropriate strain values. To reduce the influence of measurement errors included in displacement data, it is common to approximate the displacement distribution in a local region using the least-squares method and obtain strain by differentiating the approximated function.[6] Other approaches include smoothing displacement distributions using finite element models,[7,8] smoothing using spline functions,[9] and hybrid methods in which finite element analysis is performed using the obtained displacements as boundary conditions.[10] One author[11] has also proposed a method for linear elastic bodies in which boundary conditions of a finite element model are identified by inverse analysis from measured displacement distributions to obtain strain and stress.

In the case of viscoelastic bodies, when evaluating strain distributions using measurement methods such as the moiré method or digital image correlation, displacement distributions are obtained from images at each time step, and strain distributions are calculated using one of the aforementioned methods. Furthermore, to evaluate stress, it is necessary to calculate the time variation of stress from the time variation of strain at each point using viscoelastic constitutive equations. Thus, evaluation of stress in viscoelastic bodies requires smoothing the displacement distribution, differentiating it spatially to obtain strain, and then performing temporal convolution (history integration) of the strain to obtain stress. Consequently, it is difficult to achieve high accuracy due to accumulation of errors. Moreover, the use of finite element models is considered convenient for appropriately performing data processing such as spatial differentiation and temporal integration of measurement data.

Therefore, in this study, we propose a method for evaluating strain and stress in viscoelastic bodies using a DIC–FEA hybrid method that combines displacement measurements obtained by digital image correlation (DIC) with the finite element analysis (FEA). This method is an extension of a previously proposed inverse boundary identification method[11] for elastic bodies to viscoelastic bodies. In this method, boundary load values are determined by inverse analysis so that displacement distributions equivalent to those obtained by measurement are reproduced by FEA, and smooth displacement and strain distributions are obtained. Stress distributions are evaluated by numerically integrating viscoelastic constitutive equations based on the time variation of strain at each point. Although this method utilizes FEA results, displacement and strain are evaluated based on measured displacement distributions, and stress is subsequently calculated. Therefore, it is effective for problems in which reliable analysis results cannot be obtained by FEA due to unclear boundary conditions.

STRESS AND STRAIN ANALYSIS OF ELASTIC BODIES BY INVERSE BOUNDARY IDENTIFICATION

Basic Principle

Consider a linear elastic body for which in-plane displacement distributions are obtained in a measurement region by measurement methods such as the moiré method or digital image correlation. Suppose that part of the displacement in the analysis region is constrained, and a unit concentrated load $P_j = 1$ is applied at a point on the boundary. Let the displacement components at an internal point (x_i, y_i) be u'_{ij} and v'_{ij}. Here, i and j are indices for identifying measurement points and boundary load positions, respectively, where $i = 1 \sim M$ and $j = 1 \sim N$. That is, the number of concentrated loads applied on the boundary is N, and the number of displacement evaluation points in the domain is M. The displacement components u'_{ij} and v'_{ij} can be regarded as compliance representing the relationship between a load applied at a boundary point and the displacement at an interior point. If the actual boundary load values are F_j, the following relationship holds by the principle of superposition:

$$\begin{aligned} u_i &= u'_{ij} F_j \\ v_i &= v'_{ij} F_j \end{aligned} \quad (i = 1 \sim M,\ j = 1 \sim N) \tag{1}$$

where u_i and v_i are displacement components at (x_i, y_i). The displacement components u'_{ij} and v'_{ij} can be obtained by FEA, while u_i and v_i are measured values. Therefore, if $M > N$, the boundary loads F_j can be obtained by the least-squares method as follows:

$$\mathbf{F} = \left(\mathbf{A}^T \mathbf{A}\right)^{-1} \mathbf{A}^T \mathbf{U} \tag{2}$$

Here, **F**, **A**, and **U** denote the nodal forces on the boundary, the compliance matrix obtained from unit concentrated loads, and the measured displacement vector, respectively.

Once the boundary load values F_j are obtained, strain values can be obtained by the principle of superposition as follows:

$$\begin{aligned} \varepsilon_{xi} &= \varepsilon'_{xij} F_j \\ \varepsilon_{yi} &= \varepsilon'_{yij} F_j \quad (i = 1 \sim M,\ j = 1 \sim N) \\ \gamma_{xyi} &= \gamma'_{xyij} F_j \end{aligned} \tag{3}$$

where ε_{xi}, ε_{yi} and γ_{xyi} are strain components at (x_i, y_i), and the primed quantities denote components obtained when a unit load is applied at the j-th point. In this method, boundary loads are determined so that the displacement distribution matches the measured distribution. Furthermore, since the least-squares method is used considering measurement errors, the obtained results are considered to be highly reliable.

Introduction of Regularization

In the above method, the influence of measurement errors included in the input displacement leads to fluctuations in the identified boundary loads. As a result, while smooth and appropriate displacement and strain distributions are obtained inside the analysis region, some irregularities appear near the boundaries. Such phenomena are common in inverse problem analysis, and various regularization methods have been proposed.[12] In this study, we propose introducing a regularization term that minimizes the second derivative of displacement:

$$\mathbf{F} = \left(\mathbf{A}^T \mathbf{A} + \alpha \mathbf{A}_{,xx}^T \mathbf{A}_{,xx} + 2\alpha \mathbf{A}_{,xy}^T \mathbf{A}_{,xy} + \alpha \mathbf{A}_{,yy}^T \mathbf{A}_{,yy}\right)^{-1} \mathbf{A}^T \mathbf{U} \tag{4}$$

where α is the regularization parameter. By minimizing the second derivative of displacement, i.e., the variation of strain, fluctuations in strain near the boundary are reduced. As a result, appropriate strain values can be obtained not only inside the measurement region but also near the boundaries.

Extension to Viscoelastic Bodies

Consider the case where the measurement target is a linear viscoelastic body. In this case, the relationship between boundary loads and displacement varies depending on loading rate and elapsed time, and therefore it is not possible to correctly determine the boundary load values directly from the displacement distribution. On the other hand, since superposition holds for displacement and strain distributions, it is possible to obtain displacement and strain distributions by determining apparent boundary load values using the same method as for elastic bodies. However, stress values cannot be determined by superposition in the same manner as boundary loads. Therefore, after determining the time-dependent strain distribution, stress is

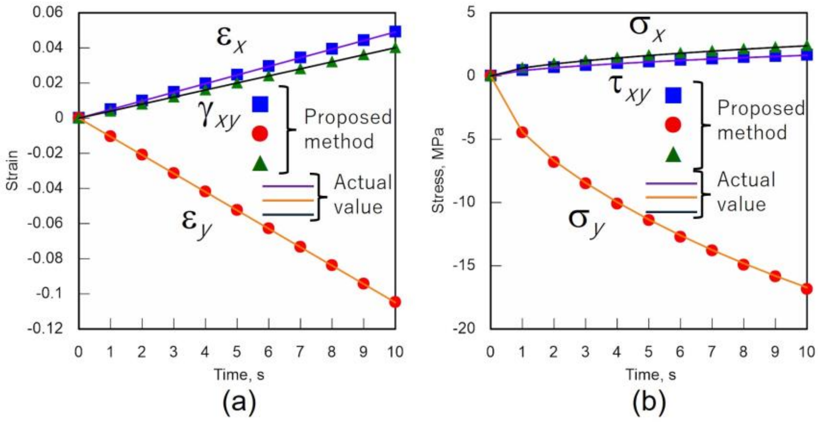

FIGURE 1: (a) Variation of strain components and (b) corresponding stress components

calculated from the temporal variation of strain at each point using viscoelastic constitutive equations.[13] Here, it is necessary to consider the time dependence of Poisson's ratio. In generating the compliance matrix **A**, analyses are performed by applying unit concentrated loads; however, if the Poisson's ratio used in this analysis is not correct, the superposition of displacements cannot be performed accurately. Since the Poisson's ratio of viscoelastic materials exhibits time dependence,[14] the displacement components u'_{ij} and v'_{ij} obtained by applying unit loads must be calculated using viscoelastic analysis, and the matrix **A** must be constructed at each time step.

Validation of Effectiveness

To validate the effectiveness of the proposed method, displacement distributions obtained by FEA are used as input in place of measured values. The viscoelastic material properties of acrylic reported by Schapery et al.[15] are used, and converted to a temperature of 463 K using the WLF time–temperature superposition principle.[16]

A constant displacement rate of 0.1 mm/s is applied to the top of the 20 mm × 10 mm model for 10 seconds. Displacement distributions within a central region of 6 mm × 6 mm are extracted every second and used as simulated measurement data. The two-dimensional finite element model consisted of 8-node quadratic elements, with 200 elements and 666 nodes. For the analysis region of 6 mm × 6 mm, a separate finite element model is constructed using 8-node quadratic elements with 36 elements and 133 nodes. The same material properties and temperature are used. Unit concentrated loads are applied in the x and y directions at boundary nodes, and viscoelastic analyses are performed to obtain time-dependent displacement and strain distributions. By repeating this procedure for different load positions and directions, the matrix **A** is constructed at each time step. The number of boundary load conditions is $N = 93$, and the number of data points is $M = 900$. Since no measurement error is assumed in this simulation, regularization is not applied.

Stress values in the proposed method are calculated from the temporal variation of strain components using history integration, where Simpson's rule is employed for numerical integration. **Figure 1** shows the time variation of strain components at a certain point and the corresponding stress components calculated from them. As shown in **Fig. 1**, the strains and stresses obtained by the proposed method agree well with the exact solutions, demonstrating that the proposed method can accurately determine strain and stress in viscoelastic bodies.

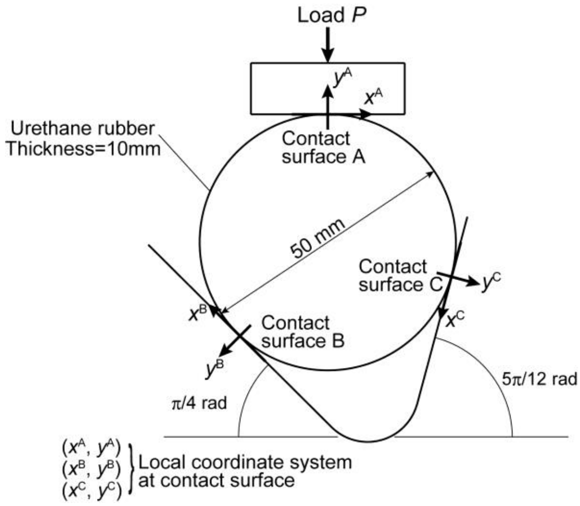

FIGURE 2: Specimen and loading condition for contact stress analysis

APPLICATION TO CONTACT PROBLEMS IN VISCOELASTIC BODIES

Experimental Method

Contact problems are generally difficult because boundary conditions at contact surfaces are not well known, resulting in low reliability of direct FEA. For example, at a contact interface, regions of slip and stick coexist, and these cannot be determined solely from a friction coefficient, making it difficult to accurately evaluate contact stress distributions.[17] In contrast, the proposed method allows boundary loads, including those on contact surfaces, to be obtained from internal measurement data through inverse analysis. That is, it becomes possible to determine load distributions on contact surfaces. In this section, an example of stress evaluation near contact regions in a viscoelastic body using the proposed method is presented.

Figure 2 shows the specimen and loading conditions used. The specimen is a circular disk made of polyurethane rubber. A random speckle pattern is applied to the specimen surface using black and white spray to enable displacement measurement by DIC. The relaxation bulk modulus and shear modulus of the material are determined using the virtual fields method.[18]

Using the loading fixture shown in the figure, three types of contact conditions—normal and shear loading—can be realized.[19] Independent coordinate systems are defined at each contact point. The experiment is conducted in a temperature-controlled chamber at 265 K, and the specimen is compressed vertically at a constant displacement rate of 0.045 mm/s. Images near the contact surface are captured at 1 frame/s using a monochrome CMOS camera with a resolution of 2048 × 2048 pixels (8-bit). A macro lens with a focal length of 200 mm and an aperture of f/11 is used. For DIC analysis, subsets of 31 × 31 pixels are used, with bicubic interpolation, a first-order shape function, and a step size of 5 pixels. Displacement and displacement gradients are obtained using the Newton–Raphson method.[20]

Experimental Results

Figure 3 shows examples of images obtained near each contact surface, displaying a region of 1600 × 1600 pixels. As shown, a region of 10 mm × 5.5 mm including the contact surface is used as the analysis area. **Figure** 4 shows the displacement distribution obtained by DIC near contact surface A at t = 40 s. Using the displacement distributions obtained every second as input, stress analysis near the contact region is performed using the proposed method. Unit concentrated loads are applied in the x and y directions at each boundary node of a finite element

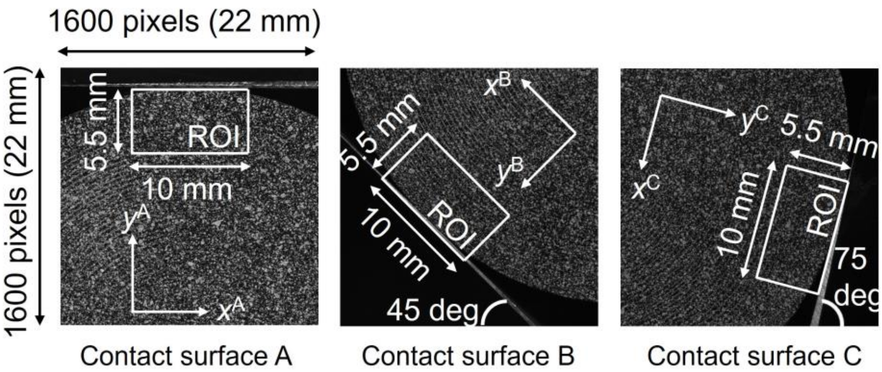

FIGURE 3: Images around contact surfaces

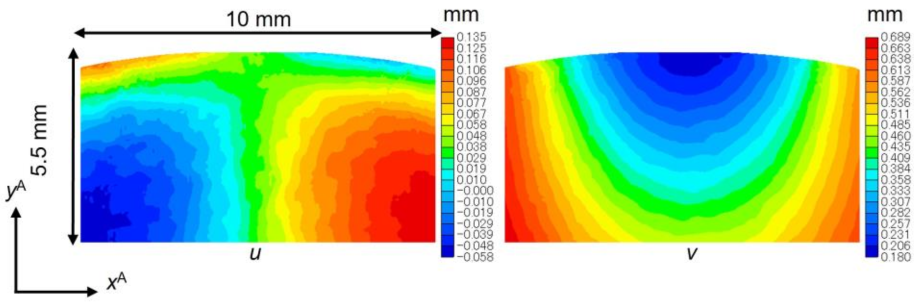

FIGURE 4: Displacement distributions around contact surface A (t = 40 s)

model, and time-dependent displacement distributions are computed to construct the matrix **A**. The regularization parameter is selected as $\alpha = 0.01$.

Figure 5 shows the strain distribution at t = 40 s and the corresponding stress distribution obtained from the temporal strain history. Since contact surface A is subjected to normal loading, the strain and stress distributions are symmetric. Although the boundary conditions of the specimen are asymmetric, the analyzed region is a local region near contact surface A and sufficiently far from other contact surfaces B and C. Therefore, the stress and strain states in this region are dominated by the boundary conditions at contact surface A, and the observed symmetry is reasonable. Focusing on the normal stress component, the maximum compressive stress does not necessarily occur at the center of the contact surface but is distributed nearly uniformly or appears slightly off-center. On the other hand, the maximum compressive strain occurs at the center. This is attributed to earlier loading initiation at the center, leading to more advanced stress relaxation compared to surrounding regions.Furthermore, in normal contact, sticking occurs at the center while slipping occurs in surrounding regions, which also influences the stress distribution.

Figure 6 shows stress distributions near contact surfaces B and C at t = 40 s. Under tangential loading, stress distributions are significantly skewed compared to those under normal loading, and exhibit complex patterns. Since stress varies significantly along the contact surface, it is inferred that regions of stick and slip coexist, similar to the case of normal contact. These regions may potentially be identified from the strain and stress distributions obtained by the proposed method, which will be investigated in future work.

CONCLUSIONS

In this study, a hybrid experimental–numerical method is proposed for obtaining strain and stress distributions in viscoelastic bodies. In this method, boundary conditions in the

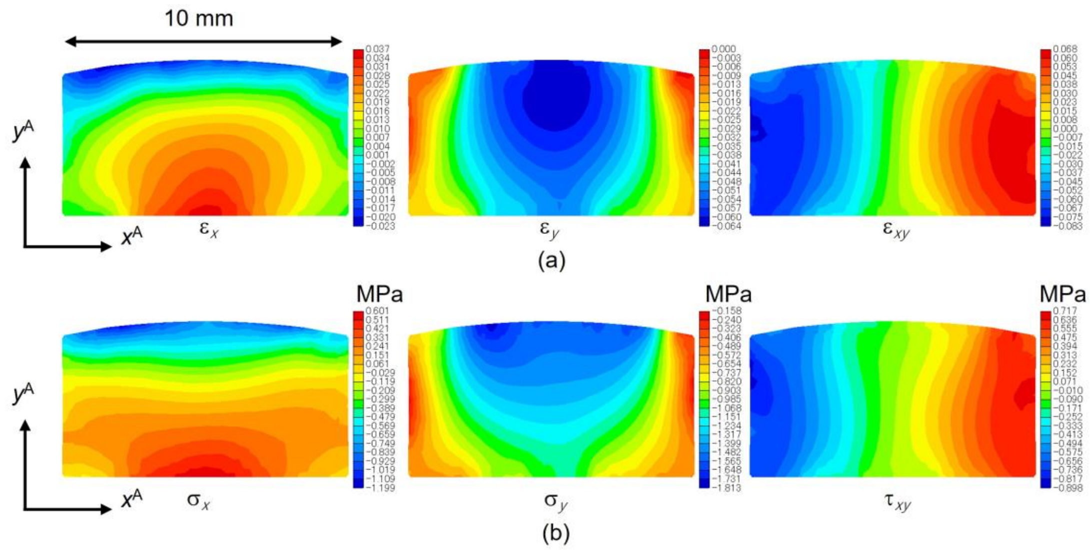

FIGURE 5: (a) Strain distributions and (b) stress distributions at contact surface A obtained by the proposed method (t = 40 s)

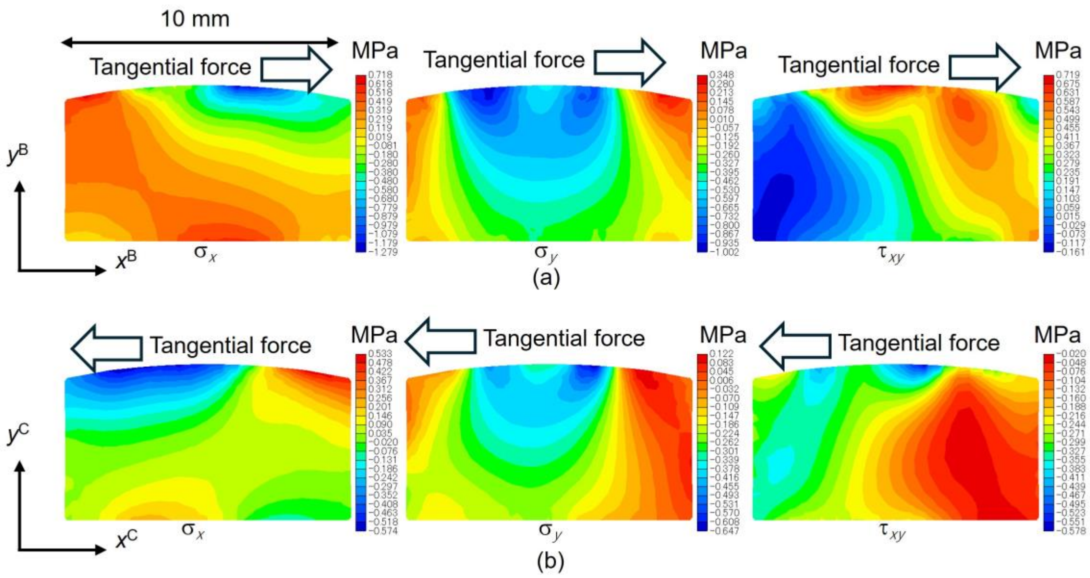

FIGURE 6: Stress distributions around (a) contact surface B and (b) contact surface C obtained by the proposed method (t = 40 s)

measurement region are determined by inverse analysis so that displacement distributions obtained by measurement are reproduced. Regularization is introduced to reduce the influence of measurement errors. As a result, strain distributions can be obtained simultaneously with displacement fields. Since stress evaluation in viscoelastic bodies requires consideration of time-dependent material properties, stress is calculated from the temporal variation of strain using history integration. As examples of the application, contact problems in viscoelastic bodies is demonstrated. In full-field measurement methods such as DIC and moiré, the measured quantity is displacement, and strain must be obtained by differentiation, which amplifies errors. In viscoelastic materials, stress must further be calculated from the temporal variation of strain, leading to cumulative errors and difficulty in achieving high accuracy. The proposed method overcomes these difficulties and is effective for stress and strain analysis of viscoelastic bodies.

ACKNOWLEDGEMENT

The authors appreciate financial support from the Research Instutite at Aoyama Gakuin University.

REFERENCES

1. Knauss, W.G. A review of Fracture in Viscoelastic Materials. *Int. J. Fract.* **2015**, 196, 99−146. https://doi.org/10.1007/s10704-015-0058-6
2. Yoneyama, S. and Takashi, M. Quantitative Characterization of Cracks and Contact Stresses Using Photoviscoelasticity. In *Advances in Mechanics of Time-Dependent Materials* (Altenbach, H., Kaplunov, J., Lu, H. and Nakada, M. eds.), Springer, 2023, 215−247. https://doi.org/10.1007/978-3-031-22401-0_13
3. Shull, K.R. Contact Mechanics and the Adhesion of Soft Solids. *Mater. Sci. Eng.* **2002**, 36, 1−45.
4 Post, D., Han, B. and Ifju, P. *High Sensitivity Moiré*. Springer, 1994.
5. Sutton, M.A., Orteu, J.-J. and Schreier, H.W. *Image Correlation for Shape, Motion and Deformation Measurement*. Springer, 2009.
6. Yoneyama, S. Computing Strain Distributions from Measured Displacements on a Three-dimensional Surface. *J. JSEM* **2010**, 10, 113−118. https://doi.org/10.11395/jjsem.10.s113
7. Segalman, D.J., Woyak, D.B. and Rowlands, R.E. Smooth Spline-like Finite-element Differentiation of Full-field Experimental Data Over Arbitrary Geometry. *Exp. Mech.* **1979**, 19, 429−437. https://doi.org/10.1007/BF02326046
8. Yoneyama, S. Smoothing Measured Displacements and Computing Strains Utilizing Finite Element Method. *Strain* **2011**, 47, 258−266. https://doi.org/10.1111/j.1475-1305.2010.00765.x
9. Sutton, M.A., Turner, J.L., Bruck, H. and Chae, T.A. Full-field Representation of Discretely Sampled Surface Deformation for Displacement and Strain Analysis. *Exp. Mech.* **1991**, 31, 168−177. https://doi.org/10.1007/BF02327571
10. Nishioka, T., Kurio, K. and Nakabayashi, H. An Intelligent Hybrid Method to Automatically Detect and Eliminate Experimental Measurement Errors for Linear Elastic Deformation Fields. *Exp. Mech.* **2000**, 40, 170−179. https://doi.org/10.1007/BF02325043
11. Yoneyama, S. and Arikawa, S. Identification of Boundary Condition from Measured Displacements for Linear Elastic Deformation Fields. *Procedia IUTAM* **2012**, 4, 215−226. https://doi.org/10.1016/j.piutam.2012.05.023
12. Kubo, S. *Inverse Problems* (in Japanese), Baifukan,1992.
13. Christensen, R.M. *Theory of Viscoelasticity*, 2nd ed., Elsevier, 1982.
14. Hoshino, Y., Tamai, K., Zhang, Y. and Yoneyama, S. Direct Measurement and Master Curve Construction of Viscoelastic Poisson's ratio with Digital Image Correlation. *Strain* **2018**, 54, e12294. https://doi.org/10.1111/str.12294
15. Parks, S.W. and Shapery, R.A. Methods of Interconversion between Linear Viscoelastic Material Functions. Part I—A Numerical Method Based on Prony Series. *Int. J. Solids Struct.* **1999**, 36, 1653−1675. https://doi.org/10.1016/S0020-7683(98)00055-9
16. Williams, M.L., Landel, R.F. and Ferry, J.D. The Temperature Dependence of Relaxation Mechanisms in Amorphous Polymers and Other Glass-forming Liquids. *J. Am. Chem. Soc.* **1955**, 77, 3701−3707. https://doi.org/10.1021/JA01619A008
17. Johnson, K.L. *Contact Mechanics*, Cambridge University Press, 1985.
18. Sun, D., Taguchi, S., Niki, I., Iizuka, K. and Yoneyama, S., The Virtual Fields Method for Identifying Viscoelastic Properties Based on Stress Sensitivity Virtual Fields. *Mech. Time-depend. Mater.* **2025**, 29, 43. https://doi.org/10.1007/s11043-025-09781-0
19. Yoneyama, S., Arikawa, S. and Kobayashi, Y. Linear and Nonlinear Algorithms for Stress Separation in Photoelasticity, *Exp. Mech.* **2012**, 52, 529−538. https://doi.org/10.1007/s11340-011-9512-1

20. Yoneyama, S. Basic Principle of Digital Image Correlation for In-plane Displacement and Strain Measurement, *Adv. Compos. Mater.* **2016**, 25, 105−123. https://doi.org/10.1080/09243046.2015.1129681